

TOWARD A PHYSICALLY-MOTIVATED DAMPING MODEL

Romain Crambuer¹, Benjamin Richard², Nicolas Ile³ and Frédéric Ragueneau⁴

¹ PhD Student, CEA, DEN, DANS, DM2S, SEMT, Laboratoire d'Etudes de Mécanique Sismique, F-91191 Gif-sur-Yvette, France. Romain.Crambuer@cea.fr

² R&D Engineer, PhD, CEA, DEN, DANS, DM2S, SEMT, Laboratoire d'Etudes de Mécanique Sismique, F-91191 Gif-sur-Yvette, France. Benjamin.Richard@cea.fr

³ R&D Engineer, PhD, CEA, DEN, DANS, DM2S, SEMT, Laboratoire d'Etudes de Mécanique Sismique, F-91191 Gif-sur-Yvette, France. Nicolas.Ile@cea.fr

⁴ Professor, Dept. of Civil Engineering, LMT, ENS-Cachan/Univ P.&M. Curie/CNRS/PRES Universud Paris, 61 Avenue du Président Wilson, F-94230 Cachan, France. Frederic.Ragueneau@lmt.ens-cachan.fr

ABSTRACT

The way of modeling the damping phenomenon in nonlinear time history analyses is still an opened question and remains a motivating challenge in the scientific community. The well-known approach lies in considering nonphysical viscous forces that are proportional to the velocity field. A damping matrix must be defined and its identification is not based on physical considerations. This study aims at exploring the possibility of identifying a local constitutive model in order to account for damping in a natural way. To reach this objective, an experimental campaign based on reinforced concrete beams subjected to reverse three- point bending tests have been performed in order to identify in an accurate way the hysteretic scheme used to take into account the hysteretic phenomenon. A specific hysteretic scheme is identified as relevant in terms of energy dissipation. Numerical free vibration tests are then carried out in order to demonstrate that the use of a viscous damping can be avoided if the local constitutive concrete model accounting for hysteretic phenomenon is accurately identified. Finally, as perspectives of this work, a method to develop a simplified physically motivated damping model is exposed and discussed.

INTRODUCTION

When considering time excitation loading applied to a mechanical system, a damping phenomenon is observed. As it appears in the analysis of the Benchmark of the nuclear structure SMART2008 that were realized by Richard et al. (2013), the way of modeling this damping phenomenon is still an opened question and remains a motivating challenge in the scientific community. Nowadays, several sources of damping have been identified and related phenomena are recognized as contributing factors to the overall damping phenomenon. In the case of concrete or reinforced concrete one can point out (i) the frictional sliding between the surfaces of the crack, (ii) the bond at the steel/concrete interface that may induce residual displacements, (iii) the radiation damping and (iv), the energy dissipation at connections or the dissipation due to non-structural components. Classically, damping is modeled in a global and non-physical way by considering additional viscous forces in the momentum balance equation. A so-called viscous damping matrix accounting for several contributing phenomena, responsible for energy dissipation is introduced. Such a damping matrix is considered for example in the engineering practice, in a design context, to describe the effects of highly dissipative phenomena such as cracking and other sources of energy dissipation. In such a case, linear or quasi-linear structural models are used to predict the time history response of a given structure. Typically 5% viscous damping ratio for concrete structures is considered to cover all sources of damping up to member yielding, including concrete cracking. The most common linear viscous damping model is the Rayleigh's damping model see Rayleigh, (1945):

$$C = \alpha M + \beta K \quad (1)$$

where C is the damping matrix, α and β are scalar parameters identified from the two first modal frequencies, M is the mass matrix and K is the stiffness matrix. A damping matrix of the form presented in (1) is also largely used in nonlinear time history analysis. Recent works by Ragueneau et al., (2000), Carr, (2004), Charney (2008) and Demarie et al. (2010), have demonstrated that the use of a viscous damping model, in the frame of nonlinear time history analyses, often leads to inaccurate estimations of displacement and internal forces in the structure. From the above discussion, it is clear that modeling the damping phenomenon properly is still nowadays not an easy task. This study aims at exploring the possibility to identify better local constitutive models in order to account for damping in a natural way, leading to a drastic reduction of the viscous damping matrix contribution. In fact, the choice of the laws used to model the damping mechanisms will have a great influence on the results of the numerical analyses. A key point is that the concrete constitutive law accounts for hysteretic phenomena. Nevertheless, the hysteretic scheme needs to be identified properly. To do so, an experimental campaign has been carried out in order to acquire appropriate experimental data related to energy dissipation in RC structural components. This campaign is based on reverse cyclic three points bending loading applied to RC beams. The experimental results are post-processed in an original way, helping to better identify local hysteretic schemes to be used in nonlinear constitutive laws. The identified model is validated at the structural scale and used to carry out a numerical campaign that consists in free vibration tests. This paper is outlined as follows. In section 2, the refined constitutive concrete model used is exposed. Formulated within the theoretical framework of the irreversible thermodynamic processes, the first and second thermodynamic principles are fulfilled. This major feature provides the physical consistency of the constitutive law. In section 3, the campaign setup is exposed and the material parameters are presented. In section 4, the experimental/numerical comparisons are presented and discussed. Then, a numerical campaign based on free vibration tests is carried out, highlighting the fact that the damping matrix can be drastically decreased when using such a refined constitutive model. The main limitation of such model come from the computational cost required that is too important, especially when probabilistic analyses should be carried out. Finally, the perspectives of this work are presented. A simplified strategy that allows a damping updating identified from the results obtained by the refined model is proposed. Although this work is still ongoing, first results are exposed and seem encouraging.

CALIBRATION OF THE REFINED CONSTITUTIVE LAW

Semi local/semi global approach: the multifiber framework

The multifiber approach allows including nonlinear constitutive laws in a finite element model built from Timoshenko's or Euler-Bernoulli's beam elements has been chosen. Indeed it allows in a relatively easy way to perform nonlinear cyclic analyze on concrete structures without paying a too heavy computational costs, moreover when parametric studies are expected as explained hereafter. A relationship between the axial strain, the curvature, the rotation and the generalized stresses represents the constitutive behavior operator. Each element cross section is described using classical two-dimensional elements (three node triangular element or four node quadrilateral element for instance). At the cross section scale, each material is characterized by a one-dimensional constitutive law linking the normal stress and the shear stresses respectively to the axial strain and to the shear strains. The major point of the multifiber approach is to add kinematic assumptions to relate the global nodal displacement (beam element) to the local strains (cross section), thanks to the well-known beam theories such as Timoshenko's or Euler-Bernoulli's theories. In the present study, the Timoshenko's beam theory is considered; the cross section remains plane but not necessarily perpendicular to the neutral axis. Therefore, considering the general case of a bending problem, for a given cross section denoted $S(x)$ at the point x and for any point at a vertical location y , local strains ε_{xx} and ε_{xy} are linked to the axial displacement $u(x)$, to the vertical displacement $v(x)$ and to the rotation $\theta(x)$ according to:

$$\varepsilon_{xx} = \frac{du(x)}{dx} - y \frac{d\theta(x)}{dx}, 2\varepsilon_{xy} = \frac{dv(x)}{dx} - \frac{d\theta(x)}{dx} \quad (2)$$

Constitutive laws

Richard's model

This study will consider a constitutive model that is expressed within the framework of isotropic continuum damage mechanics and plasticity for seismic applications and have been developed by Richard and Ragueneau. (2013). It is based on the following observations of Mazars et al. (1990). In tension, quasi-brittle materials exhibit localized cracking although in compression diffuse (or smeared) cracking appears. Therefore, isotropic damage is used in tension and plasticity is used in compression. The use of plasticity in compression is frequent in the field of soil mechanics when nonlinearities and permanent strains must be described. Tension and compression can be split into two distinct parts by considering the sign of the Cauchy stress. Since hysteretic phenomena are related to localized cracking, this mechanism is considered in tension, allowing a realistic description not only of hysteretic loops but also of permanent strains in tension. The unilateral effect is also taken into account using a closure function which ensures the continuity stress/strain relation whatever the loading path. With these assumptions, one can state that the behaviour of a representative elementary volume is accurately represented in tension (brittleness, hysteretic loops and permanent strains) and globally described in compression (nonlinearity and permanent strains). Several choices can be made to formulate a suitable thermodynamic state potential. The best known lies in expressing this potential as the Helmholtz free energy that a strain-based formulation or as the Gibbs free enthalpy, that is a stress-based formulation, Lemaitre et al. (1985). Recently, a new class of constitutive models based on a state coupling between damage and friction has been developed to describe the behaviour of quasi-brittle materials subjected to cyclic loadings see, Ragueneau et al. (2000), Richard et al. (2010). The potential can be expressed as the Helmholtz free energy, according to equation 3:

$$\rho\psi = \frac{1}{2}\{(1-d)(\varepsilon - \varepsilon^p)E(\varepsilon - \varepsilon^p) + d(\varepsilon - \eta\varepsilon^\pi - \varepsilon^p)E(\varepsilon - \eta\varepsilon^\pi - \varepsilon^p) + \gamma\alpha^2\} + H(z) + R(p) \quad (3)$$

where the ρ is the material density, ψ the Helmholtz free energy, E the Young modulus and ε is the strain, d is the scalar damage variable, ε^p is the permanent strain, η is the closure variable, ε^π is the internal sliding strain, γ is the kinematic hardening modulus, α is the kinematic hardening variable, z is the isotropic hardening variable, p is the cumulative plastic strain and H and R are two consolidation functions linked respectively to damage evolution and plastic strain evolution. The constitutive laws show interesting properties such as the representation of hysteretic loops and permanent strains. The unilateral effect is taken into account through a closure function, ensuring not only the continuity of the stress/strain relation but also a full stiffness recovery when switching from tension to compression. This criterion is expressed in terms of strain. In other words, as soon as the strain becomes negative, no internal variable is activated. Indeed, even though the strain is high and therefore, the stress is close to 0, hysteretic loops will be created when unloading, while a strain equal to 0 is not reached. The Cauchy stress can be described by equation 4:

$$\sigma = (1-d)E(\varepsilon - \varepsilon^p) + dE(\varepsilon - \eta\varepsilon^\pi - \varepsilon^p) \quad (4)$$

Menegotto and Pinto's model

The steel reinforcing steel bars are modelled by the well-known Menegotto and Pinto's constitutive law see, Menegotto et al. (1973), modified by Filippou et al. (1983). This constitutive model accounts for both isotropic and kinematic nonlinear hardenings. In particular, the Bauschinger effect can be described.

DEFINITION OF THE CAMPAIGN

Campaign specifications

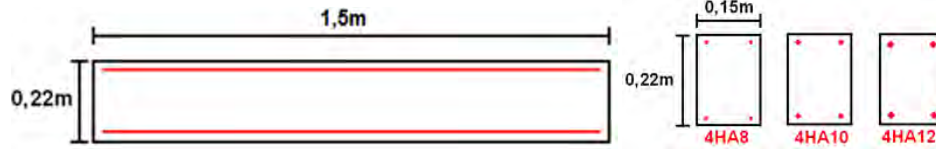


Figure 1. RC beam specimen dimensions and reinforcement detailing.

Six rectangular RC beams are tested with different longitudinal reinforcement steel ratios specification. The campaign is fully described in Crambuer et al, (2012). The reinforcement details are presented in figure 1. The concrete used is a regular one C30/37. The RC beams are designed to be tested with a simple three-point bending setup in the vertical direction up and down. The hinge device used in this campaign allows ensuring a free-rotation condition at the end supports of the beams. For each series of beams, two different loadings are applied. The aim of the loading L1 is to evaluate damping for different levels of progressive cracking. In comparison with the L1 loading, the L2 history tends to generate dissipation for a pre-cracked specimen generating progressive erosion of the cracked surfaces

Material parameters identification

Richard's model

The material parameters used in the numerical analysis are presented in table 1. They were selected according to the experimental data. To illustrate the stress/strain curve in tension, the local response obtained at the Gauss's point level is shown in figure 2(a). In particular, one can observe a brittle behaviour, the presence of inelastic strains, the unilateral effect and some hysteretic loop.

Table 1. Material parameters used for Richard's model.

| Symbol | Parameter | Identified value | Unit |
|------------|---|---------------------|--------------------|
| E | Young's modulus | $28000 \cdot 10^6$ | Pa |
| ν | Poisson's ratio | 0.2 | |
| Y_0 | Initial threshold for damage activation | 82.82 | $J \cdot m^{-3}$ |
| A_d | Brittleness coefficient | $9.0 \cdot 10^{-3}$ | $J^{-1} \cdot m^3$ |
| γ | Kinematic hardening modulus 1 | $3.0 \cdot 10^9$ | Pa |
| a | Kinematic hardening modulus 2 | $8.0 \cdot 10^{-6}$ | Pa^{-1} |
| σ_f | Mean closure stress | $-3.0 \cdot 10^6$ | Pa |
| σ_c | Compressive strength | $-10.0 \cdot 10^6$ | Pa |
| a_R | Plastic hardening modulus 1 | $4.0 \cdot 10^{10}$ | Pa |
| b_R | Plastic hardening modulus 2 | 600 | |

Menegotto and Pinto's model

The material parameters related to the Menegotto and Pinto's model used in the numerical simulations are presented in table 2. They were selected according to the experimental data. To illustrate the stress/strain response, a cyclic tension/compression loading has been simulated at the Gauss's point level. The results are shown in figure 2(b). Note that this model allows taking into account the Bauschinger effect and buckling of reinforcing bars.

Table 2. Material parameters used for Menegotto and Pinto's model.

| Symbol | Parameter | Identified value | Unit |
|-----------------|--|---------------------|------|
| E | Young's modulus | $210000 \cdot 10^6$ | Pa |
| ν | Poisson's ratio | 0.3 | |
| b | Strain-hardening ratio | 0.000877 | |
| R_0 | Control the transition from elastic to plastic branches | 20 | |
| σ_y | Yield stress | $560 \cdot 10^6$ | Pa |
| σ_u | Ultimate stress | $682 \cdot 10^6$ | Pa |
| ε_y | Yield strain | 0.0029715 | |
| ε_u | Ultimate strain | 0.534 | |
| A_1 | Isotropic hardening parameter 1 | 18.5 | |
| A_2 | Isotropic hardening parameter 2 | 0.15 | |
| A_6 | Isotropic hardening parameter 3 | 620 | |
| C | Isotropic hardening parameter 4 | 0.5 | |
| A | Isotropic hardening parameter 5 | 0.006 | |
| A_{ld} | Ratio between the shear reinforcement bar diameter and the considered bar diameter | 5 | |

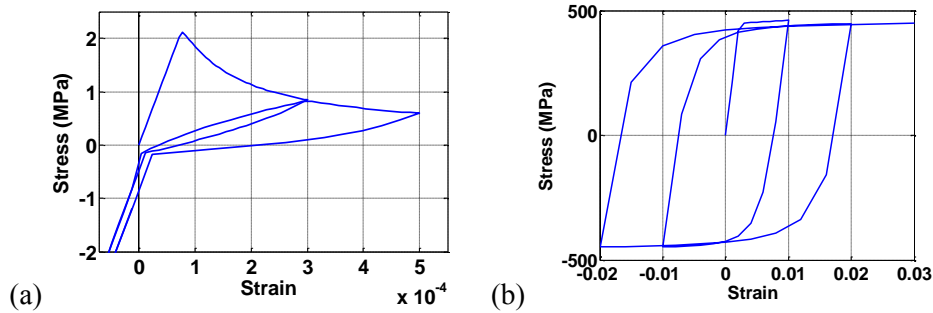


Figure 2. Stress-strain Response for concrete (a) and steel (b) with the experimental parameters

NUMERICAL RESULTS

Structural behavior of the RC beams

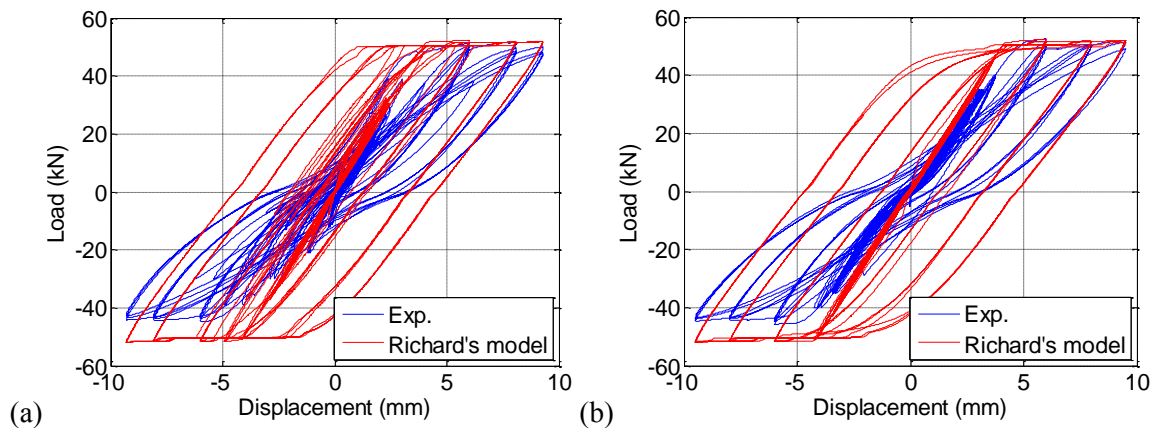


Figure 3. Load/midspan displacement curve of the beam HA10 – (a) L1 and (b) L2 loading.

Two different versions of the numerical model presented above and a reference model developed by La Borderie that doesn't include hysteretic loops were used to simulate the cyclic three-point bending tests, as you can see in Crambuer et al. (2013). The load/midspan displacement curves obtained with the best model are shown in figure 3. As expected, the numerical results obtain with the Richard's model are in satisfactory accordance with the experimental ones. One can notice that the initial stiffness is well described and that the maximum load is in most cases well estimated. The experimental results obtained with digital image correlation, using the CORELLIQ4 software, developed by Hild, (2006), are presented in figure 4. It can be observed that when the applied load is close to 0 kN, the cracks are opened on both sides of the beam. At the structural level, this is the expression of the fact that the beam stiffness is close to zero (horizontal tangent). Note that the same experimental measures have been carried out for each RC beam. However the model is not able to capture this effect that appears for the last cycles. The beam kinematics imposed in the analysis prevents one to account for complete 2D behaviour and local bond-slip degradation between steel and concrete. Such a lack in the description may explain such results.

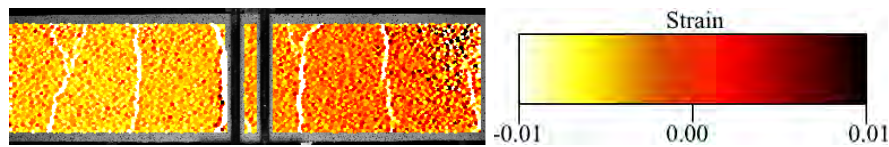


Figure 4. Horizontal strain for an applied load of 0 of the beam HA10L2 - ±6mm displacement cycle

Equivalent viscous damping ratio

In order to study the capability of each model to dissipate energy when considering cyclic loading, the numerical and the experimental equivalent viscous damping ratios, developed by Jacobsen (1960), and Varum (2003) are compared with each other in figure 5. The Richard's model allows obtaining good results in both loadings whereas the reference model was not able to model equivalent viscous damping ratios. It confirms that the damping in concrete is generated by the hysteretic loops. In the case of the low level of loading, the dissipation may come from the hinge device and some compression near the loading system. Based on these results, one can state that the Richard's model seems to be calibrated suitably not only in terms of load/midspan displacement but also in terms energy dissipation related to the hysteretic effects.

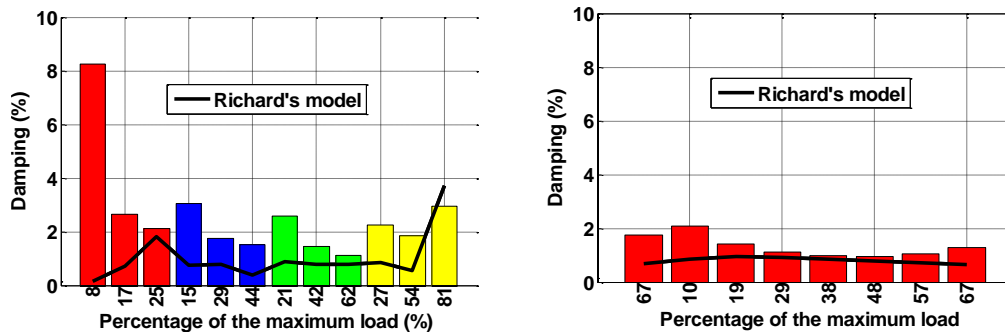


Figure 5. Equivalent viscous damping ratio/normalized load curves – beam HA10 – L1 and L2 loading.

Numerical free vibration tests

In this section, the capabilities of the Richard's model to generate damping without considering a viscous damping matrix are studied. To achieve this goal, numerical free vibration tests have been

simulated considering the material parameters that have been identified previously. Such studies have been realized by Desmorat et al, (2007). The RC beam with HA12 reinforcement steel bars is considered. Since, similar results have been obtained with other RC beams, they are not presented here for brevity. As it has been identified from the experimental results presented in previous section., the equivalent viscous damping ratio related to the energy dissipation of concrete cracking is about to 2%. Therefore, a reference model with linear elastic constitutive law for concrete and steel has been defined. The damping is modeled by the well-known Rayleigh approach. Assuming a 2.0% critical damping factor for the first and second vibration mode, the damping parameters were calculated and used subsequently to form the Rayleigh damping matrix $[C] = \alpha[M] + \beta[K]$, M and K being the mass and stiffness matrix.

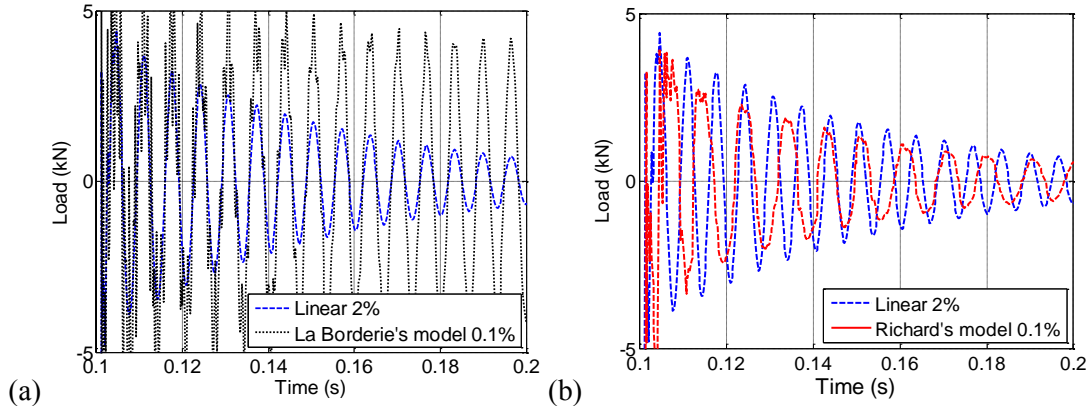


Figure 6. Load/time results – initial load applied equal to 40 kN – (a) La Borderie’s (b) Richard’s model.

The numerical results obtained by this reference model when simulating free vibration tests are compared with those obtained by the La Borderie and Richard’s models. Note that in the case of La Borderie and Richard’s models, the contribution of the damping matrix is very low since the coefficients have been calibrated to obtain a critical damping factor equal to 0.1% on the first and second vibration mode for numerical robustness reasons. The loading is load-controlled. The maximum load is equal to 40 kN, that correspond to 60% of the beam capacity, and is applied at midspan. The load/time results are presented in figures 6(a) and (b). In the case of the La Borderie model, it clearly appears that without considering a significant viscous damping matrix, the oscillations of the RC beam cannot be damped. This is mainly due to the fact that no hysteretic effect is taken into account in the model. On the opposite, in the case of the Richard’s model, the damping level obtained is similar to the one obtained by the reference model. This result shows that the damping phenomenon can be modeled in a physical way since the constitutive laws describe reasonably well the main sources of dissipation. Furthermore, it can be stated that the contribution of the viscous damping matrix can be drastically reduced in this way.

FUTURE RESEARCH CONTENT

Aims

In this study, it has been shown that the use of a refine constitutive law could lead to drastic reduction of the contribution of the viscous damping matrix that is not physically motivated. Nevertheless, the computational cost required when using such models remains high when probabilistic analyses should be carried out. The main perspective of the work that has been exposed in this paper lies in proposing a simplified strategy that allows a damping updating identified from the results obtained by the refine model. The new model will be called DBSM model because, in this Simplified Model, the damping C is updated according to the evolution of a damage variable D . The methodology is the following one:

- calibration of the refine model based on the three-point bending tests,

- simulation of numerical homogeneous bending tests to build a damage/damping ratio relation,
- implementation of the damage/damping ratio relation in a structural 1D constitutive law,
- validation of the proposed strategy on a real experimental campaign.

Simulation of homogeneous bending numerical test

According to the previous works, it has been shown that the Richard's model is able to quantify the dissipated energy of a structure. In order to quantify the dissipated energy for a given damage level, numerical homogeneous bending tests have been performed. Such loading generates homogeneous strain fields and so, homogeneous damage fields that allows defining a damage level at the member scale. The loading lies in symmetric cycles of increasing intensity. Each cycle gives a good estimation of the dissipated energy $E_D^{Richard's}$ by the structure for a given damage level.

Implementation and energy balance

The proposed simplified model is a single degree of freedom oscillator in which the damping ratio is updated according to the damage level. In order to build a damage/damping ratio relation in a structural 1D constitutive law, the dissipation of this model must be quantified. To do so, the well-known equations that govern the dynamic behavior of a 1D oscillator under free vibration are considered: the equilibrium equation (5), the constitutive law (6) and the kinematic law (7).

$$m\ddot{u}(t) + c\dot{u}(t) + (1 - D)Ku(t) = 0 \quad (5)$$

$$f = (1 - D^+)Ku^+ + (1 - D^-)Ku^- \quad (6)$$

$$u(t) = \lambda e^{st} \quad (7)$$

$$\text{With : } \ddot{u}(0) = 0 \quad \dot{u}(0) = 0 \quad u(0) = u_0 \quad \ddot{u}(\infty) = 0 \quad \dot{u}(\infty) = 0 \quad u(\infty) = 0 \quad (8)$$

where m , c , f , D^+ , D^- , K and r are respectively the mass, the damping, the force, the two damage variable and the elastic stiffness and the stiffness of the system, \ddot{u} , \dot{u} and u are respectively the acceleration, velocity and displacement of the structure, u^+ and u^- are respectively the negative and positive part of the displacement, λ and s are parameters. From this system of equations the displacement can be described as:

$$u(t) = \left[\frac{\dot{u}(0) + \xi \omega u(0)}{\omega_D} \sin(\omega_D t) + u(0) \cos(\omega_D t) \right] e^{-\xi \omega t} \quad (9)$$

$$\text{with: } \omega_D = \omega \sqrt{1 - \xi^2} \quad \xi = \frac{c}{2\sqrt{k_d m}} \quad \omega = \frac{k_d}{m} \quad K_D = (1 - D)K \quad (10)$$

where ω and ω_D are respectively the natural frequency and the damped natural frequency, ξ is the critical damping ratio and K_D the secant stiffness of the system. Then the dissipated energy E_D^{DBSM} can be expressed for a given damage level as:

$$E_D^{DBSM} = \int_0^\infty c\dot{u}(t)du \quad (11)$$

After some calculations the dissipated energy could be expressed as:

$$E_D^{DBSM} = -c \cos(\varphi) m(1 + \xi) \left(\cos(\varphi) + \frac{\omega_D}{\xi(1-\xi)^2} - \frac{\sin(\varphi)}{(1-\xi)^2} \right) \quad (12)$$

$$\text{with: } \varphi = \tan^{-1} \left(\frac{\omega_D}{\xi} \right) \quad (13)$$

where φ is the phase shift.

In order to dissipate a realistic energy the damping ratio ξ must be fit to respect the equality:

$$E_D^{DBSM} = E_D^{Richard's} \quad (14)$$

If the same calculations are performed for a significant number of damage levels a relation between the damping ratio and the damage ratio can be established, for a given reinforced steel ratio, as presented figure 8.

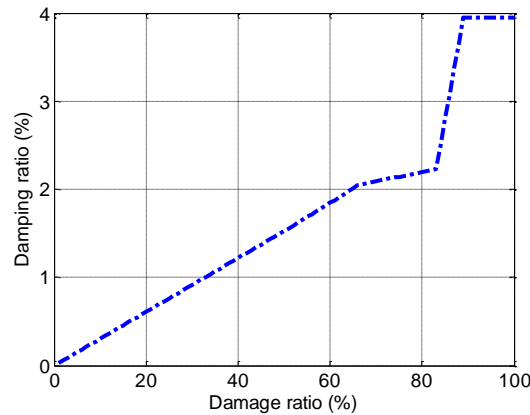


Figure 8. Damage/Damping curve for a steel reinforcement ratio of 1%.

Validation

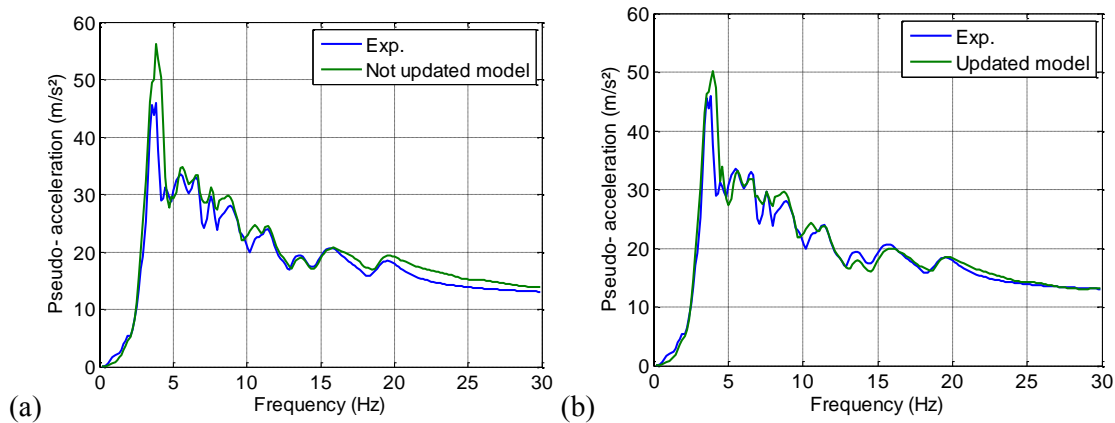


Figure 9. Pseudo acceleration at the top/frequency curve of the SIBA column – 0.45 run.

The DBSM model has been used to model the behavior of a RC column. This column was a part of the experimental campaign SIBA. This campaign aims in studying the influence of shear reinforcement on columns of various heights submitted to 1D seismic loads. This column is 1.5m tall with a section of 0.17 x 0.25m. Six 1D seismic loads have been applied to this structure. Figure 9 presents a comparison between the experimental and numerical horizontal pseudo-acceleration of the top of the column for the third run in order to compare the frequency content. This run generates a high level of damage but no yielding. On figure 9(a) the damping updating is not taken into account by the model contrary to the results present in 9(b). Both models are able to catch the eigen frequency but only the updated model gives an accurate pseudo-acceleration. This suggests that such methods could lead to a good and physical

evaluation of the damping ratio of the structure without modeling the physical phenomenon at the material scale. Nevertheless this work is limited to the analyses of a SDOF structure submitted to a 1D seismic load have been studied. The next step will be to implement the relation between the damping ratio and the damage ratio in MDOF structure modeled with more than one element.

REFERENCES

- Carr, A. J. (1994) “Dynamic Analysis of Structures”, *Bulletin of the New Zealand National Society for Earthquake Engineering*, **271**(2), 129-146.
- Crambuer, R., Richard, B., Ile, N. and Ragueneau, F. (2012), “Experimental characterization and modelling of energy dissipation in reinforced concrete beams subjected to cyclic loading”, *Proc., 14th World Conference of Earthquake Engineering*, Lisbon, Portugal, 2913.
- Crambuer, R., Richard, B., Ile, N. and Ragueneau, F. (2013), “Characterization and modeling of energy dissipation in reinforced concrete beams subjected to cyclic loading”, *Engineering structure*, in submission
- Charney, F. A. (2008) “Unintended consequences of modelling damping in structure”, *Journal of structural engineering*, **134**(4), 581-592.
- Demarie, G.V., Sabia, D. (2010), “Non-linear damping and frequency identification in a progressively damaged R.C. element”, *Experimental mechanics*, **51**, 229-245.
- Desmorat, R., Ragueneau, F., Pham, T.H. (2007), “Continuum damage mechanics for hysteresis and fatigue of quasi-brittle materials and structures”, **31**(2), 307-329.
- Filippou, FC, Popov, EP, Bertero, VV. (1983), “Effects of bond deterioration on hysteretic behavior of reinforced concrete joints”, *Internal Report No. UCB/EERC-83/19*, Earthquake engineering research center. Berkeley: University of California.
- Hild, F, Roux S. (2006), “Measuring stress intensity factors with a camera: Integrated digital image correlation I-DIC”, *Comptes Rendus Mécanique*, **334**(1), 8-12.
- Jacobsen, L. S. (1960). “Damping in composite structures”, *Second World Conference on Earthquake Engineering*. Tokyo and Kyoto, Japan, **Proc. 2**, 1029–1044.
- Lemaître, J., Chaboche, J.L., and Germain, P., (1985) “Mécanique des matériaux solides”, Dunod.
- Mazars, J., Berthaud, Y., and Ramtani, S. (1990), “The unilateral behaviour of damaged concrete”, *Engineering Fracture Mechanics*, 35(4-5), 629–635.
- Menegotto, M., and Pinto, P. E. (1973), “Method of analysis for cyclically loaded reinforced concrete plane frames including changes in geometry and non-elastic behavior of elements under combined normal force and bending.” *IABSE Symp. of Resistance and Ultimate Deformability of Structures Acted on by Well-Defined Repeated Loads*, Lisbon, Portugal, **Proc. 13**, 15-22.
- Ragueneau, F., La Borderie, C., and Mazars, J. (2000) “Damage model for concrete-like materials coupling cracking and friction, contribution towards structural damping: first uniaxial applications”, *Mechanics of Cohesive-frictional Materials*, 5(8), 607–625 .
- Rayleigh, lord (Strutt JW) (1945), “The Theory of Sound” Dover, New York, 2nd edition, Original publication 1877, **1**(80, 81).
- Richard, B., Ragueneau, F., Cremona, C., and Adelaide, L. (2010), “Isotropic continuum damage mechanics for concrete under cyclic loading : Stiffness recovery, inelastic strains and frictional sliding”, *Engineering Fracture Mechanics*, 77(8), 1203–1223.
- Richard, B. and Ragueneau, F. (2013), “Continuum damage mechanics based model for quasi brittle materials subjected to seismic loadings: formulation, numerical implementation and applications”, *Engineering Fracture Mechanics*, 98, 383-406
- Richard B., Juster Lermite S., Chaudat T., Crambuer R., Voldoire F. and Abouri S. (2013) “SMART 2008 International Benchmark overview”, *Journal of Earthquake Engineering*, in submission
- Varum, H. (2003), “Seismic assessment, strengthening and repair of existing buildings”, *P.H.D. Thesis*, Aveiro : Civil engineering department, University of Aveiro.